BIOCHEMISTRY
including biophysical chemistry & molecular biology

Article

pubs.acs.org/biochemistry

Interaction of Profilin with the Barbed End of Actin Filaments

Naomi Courtemanche[†] and Thomas D. Pollard*[,†,‡,§]

[†]Department of Molecular Cellular and Developmental Biology, [‡]Department of Molecular Biophysics and Biochemistry, and [§]Department of Cell Biology, Yale University, P.O. Box 208103, New Haven, Connecticut 06520-8103, United States

Supporting Information

ABSTRACT: Profilin binds not only to actin monomers but also to the barbed end of the actin filament, where it inhibits association of subunits. To address open questions about the interactions of profilin with barbed ends, we measured the effects of a wide range of concentrations of *Homo sapiens* profilin 1 on the rate of elongation of individual skeletal muscle actin filaments by total internal reflection fluorescence microscopy. Much higher concentrations of profilin were required to stop elongation by AMP-PNP-actin monomers than ADP-actin monomers. High concentrations of profilin depolymerized barbed ends at a rate much faster than the spontaneous dissociation rates of Mg-ATP-, Mg-AMP-PNP-, Mg-ADP-P_i-, and Mg-ADP-actin subunits. Fitting a thermodynamic model to these data allowed us to determine the affinities of profilin and profilin-actin for barbed ends and the influence of the nucleotide bound to actin on these interactions. Profilin has a much higher affinity for ADP-actin filament barbed ends (K_d = 1 μM) than AMP-PNP-actin filament barbed ends (K_d = 226 μM). ADP-actin monomers associated with profilin bind to ADP-actin filament barbed ends 10% as fast as free ADP-actin monomers, but bound profilin does not affect the rate of association of AMP-PNP-actin monomers with barbed ends. The differences in the affinities of AMP-PNP- and ADP-bound barbed ends for profilin and profilin-actin suggest that conformations of barbed end subunits differ from those of monomers and change upon nucleotide hydrolysis and phosphate release. A structural model revealed minor steric clashes between profilin and actin subunits at the barbed end that explain the biochemical results.

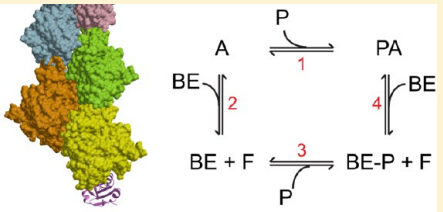

The small protein profilin performs many roles in cytoskeletal dynamics through interactions with actin monomers, poly-L-proline ligands including formins, and the barbed ends of actin filaments.[1] Understanding the mechanism of action of profilin has proven to be remarkably challenging for such a small protein (125−137 amino acids). Profilin binds actin monomers and inhibits spontaneous assembly of actin polymers,[2−5] so the initial hypothesis was that profilin sequesters actin monomers so they cannot polymerize. Low concentrations of profilin strongly inhibit actin filament nucleation[2−4] and elongation of actin filament pointed ends.[6] Both effects are due to binding of profilin to the barbed end of the actin monomer with micromolar affinity and physically blocking association of the complex with pointed ends during nucleation and elongation.[7,8]

On the other hand, events at the barbed end of actin filaments are less clear.[9] Saturating ATP-actin monomers with profilin has little effect on the elongation of actin filament barbed ends, but because high concentrations of profilin slow elongation,[6,10] profilin was proposed to bind weakly to barbed ends, thereby blocking association of subunits on the barbed end. If this filament capping mechanism is correct, theory predicts that high concentrations of profilin will stop and reverse barbed end elongation.[11] Although this was not achieved with the highest profilin concentrations used in initial studies conducted in the presence of actin monomers,[6,12−18] high concentrations of profilin depolymerized aged filaments assembled from ATP-actin and observed with DNase-I bound to actin monomers in solution[15] or diluted to lower the concentration of monomers.[19] These filaments were thought to be composed of ADP-actin subunits. Recent elegant experiments confirmed that profilin depolymerizes individual aged actin filaments in a concentration-dependent manner.[20] However, these experiments did not include actin monomers, so the rates of profilin binding and dissociation at barbed ends, the rate of dissociation of profilin-actin from barbed ends, and the overall thermodynamics of the system remained to be determined.[9]

Here we used fluorescence microscopy to test the effects of a wide range of concentrations of human profilin 1 on the elongation of skeletal muscle actin filaments by Mg-ATP-, Mg-AMP-PNP-, Mg-ADP-P_i-, and Mg-ADP-actin subunits. Low concentrations of profilin inhibited elongation of actin filament barbed ends, and high concentrations of profilin caused barbed ends to depolymerize at rates much faster than spontaneous dissociation rates. A thermodynamic analysis of the dependence of elongation rates on profilin concentration yielded the affinities of profilin for barbed ends and the influence of the nucleotide bound to actin on its interactions with profilin. Profilin has a relatively high affinity (K_d = 1 μM) for ADP-actin filament barbed ends and a low affinity (K_d = 226 μM) for AMP-PNP-actin filament barbed ends, opposite to the relative affinities of profilin for actin monomers with these bound nucleotides. Association of profilin with actin monomers slows the association of ADP-actin monomers with barbed ends but has no effect on the rate of association of AMP-PNP-actin monomers with

Received: May 29, 2013
Revised: August 13, 2013
Published: August 15, 2013

   dx.doi.org/10.1021/bi400682n | *Biochemistry* 2013, 52, 6456−6466

barbed ends. Profilin bound to a barbed end increases the dissociation rate of the terminal subunit.

MATERIALS AND METHODS

Actin Purification and Labeling. Muscle actin was purified from an acetone powder of frozen chicken skeletal muscle (Trader Joe's) using one cycle of polymerization and depolymerization followed by gel filtration on Sephacryl S-300 and storage in Ca-Buffer-G [2 mM Tris-HCl (pH 8.0), 2 mM ATP, 0.1 mM $CaCl_2$, 1 mM NaN_3, and 0.5 mM DTT].[21] The concentration of actin was measured by absorbance at 290 nm with an extinction coefficient of 26600 M^{-1} cm^{-1}.[22] Muscle actin filaments in 50 mM PIPES (pH 6.8), 50 mM KCl, 0.2 mM $CaCl_2$, and 0.2 mM ATP were labeled on lysines by being incubated overnight at 4 °C with a 1:13 molar ratio of actin to Alexa Fluor 488 carboxylic acid succinimidyl ester (A-20000, Invitrogen, Carlsbad, CA).[23] After depolymerization, clarification, and gel filtration on Sephacryl S-300, purified actin monomers were typically ~30−50% labeled. Ca-ATP-actin was converted to Mg-ATP-actin by addition of 0.1 volume of 2 mM EGTA and 500 μM $MgCl_2$ and incubation of the sample for 5 min at room temperature. Ca-ATP-actin monomers in Ca-Buffer-G were converted to Mg-ADP-actin monomers by being incubated with 50 μM $MgCl_2$, 250 μM EGTA, 1 mM glucose, and 0.25 unit/mL hexokinase (catalog no. H-2005, Sigma, St. Louis, MO) for 3 h on ice followed by clarification for 1 h at 125000*g*.[24] Mg-ADP-P_i-actin solutions were generated during total internal reflection microscopy experiments by mixing Mg-ADP-actin monomers with ADP-P_i-TIRF buffer containing 12.5 mM potassium phosphate. Mg-AMP-PNP-actin monomers were generated by two rounds nucleotide exchange with AG 1-X4 resin (Bio-Rad, Hercules, CA) followed by incubation with 1 mM AMP-PNP (catalog no. A-2647, Sigma) for 30 min at room temperature.

Profilin Purification. *Homo sapiens* profilin 1 was expressed in *Escherichia coli* BL21(pLysS) using a pMW172 plasmid[25] and purified by affinity chromatography on poly-L-proline coupled to Sepharose 4 Fast Flow (catalog no. 17-0981-01, Amersham Pharmacia, Piscataway, NJ).[26,27] We used an extinction coefficient of 15000 M^{-1} cm^{-1} at a λ of 280 nm to measure the concentration of profilin.

Microscopy and Data Analysis. Open-ended glass flow chambers were prepared as described previously.[28] Before the introduction of actin, each chamber was incubated for 1 min with two washes of 8 μL of 0.5% Tween 80 in high-salt TBS (HS-TBS) [50 mM Tris-HCl (pH 7.5) and 600 mM KCl], followed by two washes with 10 μL of HS-TBS, two 30 s incubations with 8 μL of 250 nM NEM-inactivated skeletal muscle myosin, two washes with 10 μL of HS-TBS, and two 30 s incubations with 8 μL of 10% (w/v) BSA in HS-TBS.

The standard microscopy buffer consisted of 10 mM imidazole (pH 7.0), 50 mM KCl, 1 mM $MgCl_2$, 1 mM EGTA, 15 mM glucose, 50 mM DTT, 0.02 μM $CaCl_2$, 20 μg/mL catalase, 100 μg/mL glucose oxidase, 0.5% methylcellulose [4000 cP at 2% (w/v)], and an appropriate nucleotide (0.3 mM ATP for ATP-actin, 0.37 mM AMP-PNP for AMP-PNP-actin, 0.3 mM ADP and 10 units/mL hexokinase for ADP-actin, or 0.4 mM ADP, 12.5 mM potassium phosphate, and 20 units/mL hexokinase for ADP-P_i-actin).

Polymerization was initiated by introducing actin in microscopy buffer into the chamber. Once short filaments had appeared, the solution in the chamber was replaced with a fresh sample of proteins (actin, actin with profilin, or profilin alone) in microscopy buffer and imaging was continued.

We generated time-lapse movies of growing or shortening actin filaments using prism-style total internal reflection fluorescence microscopy on an Olympus IX70 inverted microscope and a Hamamatsu C4742-95 CCD camera controlled by MetaMorph (Molecular Devices, Downingtown, PA).[29] Specimens were illuminated for 0.5−1 s at intervals of 5, 10, or 20 s depending on the rates of growth or shortening. Images were processed with ImageJ (http://rsbweb.nih.gov/ij/). For each sample, we measured the rates of barbed end elongation of 10−15 filaments, typically over a span of at least 300 s.

Molecular Models of Binding of Profilin to Actin Filament Barbed Ends. The structure of human profilin 1 [Protein Data Bank (PDB) entry 1FIK] was superimposed and compared to that of bovine profilin bound to bovine β-actin (PDB entry 1HLU). The secondary structures were then used to superimpose the actin in this model onto the two terminal subunits of an actin filament[30] to look for steric clashes between profilin and subunits within the filament. Molecular models were constructed using the program superpose[31] and other tools from the CCP4 software suite.[32] Solvent-excluded surfaces were constructed using MSMS with a probe radius of 1.4 Å.[33] Figures were made using Molscript[34] and Raster3D.[35]

Theory. In a system with actin monomers, profilin, and actin filaments, one must consider four reactions (Figure 1), identical to those used by Kinosian et al. in their analysis.[15]

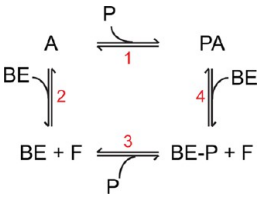

Figure 1. Thermodynamic scheme of actin filament elongation in the presence of profilin. Four reactions are depicted and labeled as follows: (1) reaction of profilin (P) with an actin monomer (A), (2) reaction of an actin monomer with the barbed end of a filament (BE), (3) reaction of profilin with the barbed end of a filament, and (4) reaction of the profilin-actin complex (PA) with the barbed end of a filament. F represents the newly incorporated filamentous subunit upon binding of actin or profilin-actin to the barbed end. BE-P represents the profilin-bound barbed end. To satisfy a detailed balance, the sum of the free energies of reactions 1 and 4 must be equal to the sum of the free energies of reactions 2 and 3. Table 2 lists the thermodynamic and kinetic parameters for AMP-PNP-actin, ADP-P_i-actin, and ADP-actin.

Reaction of Profilin with Actin Monomers. The interaction of profilin (P) with an actin monomer (A) is a simple bimolecular reaction of profilin with the barbed end of an actin monomer, creating a 1:1 profilin-actin (PA) complex.

$$A + P \leftrightarrows PA \qquad \text{(reaction 1)}$$

The rate and equilibrium constants (K_{d1}) are known for each actin-nucleotide species (Table 2). The affinity of profilin for ATP-actin in polymerization buffer is reasonably high (K_d = 0.1 μM), and the exchange rate is fast (1.3 s^{-1}).[36] The affinity of profilin for ADP-actin is ~6-fold lower.

Reaction of Actin Monomers with the Barbed Ends of Actin Filaments. Free actin monomers can bind and dissociate at both the barbed end (BE) and pointed end (PE), although the rates of the reactions differ. The association reaction converts an actin monomer (A) into a filamentous actin subunit (F), and

dx.doi.org/10.1021/bi400682n | *Biochemistry* 2013, 52, 6456−6466

the dissociation reaction converts a filamentous subunit (F) into a monomer (A). These reactions only occur at the ends of filaments, which act as catalysts and are not consumed. For the purposes of this study, we consider only subunit addition at the barbed end.

$$A + BE \leftrightarrows F + BE \quad \text{(reaction 2)}$$

The rate and equilibrium constants (K_{d2} = critical concentration) are known for ATP-, ADP-P_i-, and ADP-actin (Table 2). We measured these constants for AMP-PNP-actin in this study.

Reaction of Profilin with Actin Filaments. Profilin does not bind along the length of actin filaments in pelleting[12] or fluorescence anisotropy assays,[37] but polymerization experiments[6,10,15,18] suggested that profilin binds to the barbed ends but not the pointed ends of actin filaments. These results, combined with our structural analysis (see Figure 5), indicate that each filament has a single profilin binding site, located at the barbed end of the terminal subunit.

$$P + BE \leftrightarrows BE{-}P \quad \text{(reaction 3)}$$

Neither the rate nor equilibrium constants (K_{d3}) are known for any actin-nucleotide species. Note that our structural analysis shows that a barbed end associated with profilin (BE-P) is capped, so it cannot bind an actin monomer or profilin-actin complex. Profilin can dissociate from the barbed end alone (reaction 3) or in association with an actin subunit (reaction 4).

Reaction of the Profilin-Actin Complex with the Barbed Ends of Filaments. Profilin-actin (PA) cannot bind to the pointed end but associates with barbed ends.

$$PA + BE \leftrightarrows BE{-}PA \leftrightarrows F + BE{-}P \quad \text{(reaction 4)}$$

This association reaction consumes a barbed end and adds a subunit (F) to the filament. Note that profilin can also dissociate on its own from BE-P, yielding P and BE (reaction 3). We measured the rate constants for the dissociation of profilin-actin (PA) from barbed ends for four actin-nucleotide species (Table 1), but none of the association rate constants or equilibrium constants (K_{d4}) were known.

Table 1. Initial Rates of Barbed End Depolymerization (subunits per second) with 0 or 750 μM Profilin

	ATP-actin	AMP-PNP-actin	ADP-P_i-actin	ADP-actin
no profilin	1.4 ± 0.8[b]	2.0 ± 0.3[a]	0.2 ± 0.1[c]	5.4 ± 0.14[c]
750 μM profilin	30.3 ± 3.3[a]	52.4 ± 4.9[a]	8.6 ± 1.1[a]	12.2 ± 2.8[a]

[a]Rates measured in this study. The ATP-actin rate is the initial depolymerization rate. [b]See ref 40. [c]See ref 39.

We used the dependence of the filament elongation rates on profilin concentration to estimate the missing equilibrium constants for the affinities of profilin (K_{d3}) and profilin-actin (K_{d4}) for the barbed ends of filaments composed of subunits with different bound nucleotides. Equations 1−3 describe the evolution of the concentrations of filamentous actin (F), filament barbed ends (BE), and profilin (P) over time. These equations are based on reactions 1−4 and use the association (k_n^+) and dissociation rate constants (k_n^-) for reaction n:

$$\frac{d[F]}{dt} = k_2^+[BE][A] + k_4^+[BE][PA] - k_2^-[BE] - k_4^-[BE\text{-}P] \quad (1)$$

$$\frac{d[BE]}{dt} = k_3^-[BE\text{-}P] + k_4^-[BE\text{-}P] - k_3^+[BE][P] - k_4^+[BE][PA] \quad (2)$$

$$\frac{d[P]}{dt} = k_1^-[PA] + k_3^-[BE\text{-}P] - k_1^+[A][P] - k_3^+[BE][P] \quad (3)$$

Our experimental conditions allowed us to use four simplifying assumptions. (i) The change in the concentration of polymerized actin over time is much smaller than the initial concentration of actin monomers, so the concentrations of actin ([A]), profilin ([P]), and profilin-actin ([PA]) were constant. (ii) The total concentration of profilin does not change over time, so the initial concentration of profilin, $[P]_0$, is equal to the sum of the concentrations of free, actin-bound, and barbed end-bound profilin ([P] + [PA] + [BE-P]) at any given time. (iii) The number of barbed ends does not change over time, so the initial concentration of barbed ends, $[BE]_0$, is equal to the sum of the concentrations of free and profilin-bound barbed ends, [BE] + [BE-P], at any time. This assumption is reasonable given that our measurements were made on individual filament barbed ends. (iv) The initial concentration of actin, $[A]_0$, is equal at any time to the sum of the concentrations of free actin ([A]), profilin-bound actin ([PA]), and actin that becomes filamentous ([F]) after the start of the experiment (not including preformed filaments).

Using eqs 1−3 and our simplifying assumptions, we modified eq 1 to describe the filament elongation rate in terms of the initial concentrations of actin, profilin, and barbed ends, dissociation equilibrium constants for reactions 2−4 (K_{dn}, defined as k_n^-/k_n^+ for reaction n), and the association rate constant for reaction 2 (k_2^+):

$$\frac{d[F]}{dt} = k_2^+[BE]_0 \frac{[A]_0(K_{d3} + K_{d4}) + [P]_0(K_{d2} - K_{d4})}{[P]_0 + K_{d3} + K_{d4}} \quad (4)$$

The only unknowns are K_{d3} and K_{d4}.

RESULTS

We used total internal reflection fluorescence microscopy[29,38,39] to investigate the effects of a wide range of concentrations of human profilin 1 on actin monomer association and dissociation rates at barbed ends of actin filaments with ATP, AMP-PNP, ADP-P_i, or ADP bound to the actin monomers (Figure 2). Analysis of these polymerization data and structural models showed that profilin inhibits elongation of barbed ends by binding the terminal subunit of the filament and blocking subunit addition.

Effect of the Bound Nucleotide on Barbed End Elongation and Shortening Rates in the Absence of Profilin. To analyze our experiments with profilin, we used published barbed end association and dissociation rate constants for ATP-, ADP-P_i-, and ADP-actin monomers.[39,40] To determine association and dissociation rates for AMP-PNP-actin monomers, we visualized barbed end elongation rates over a range of monomer concentrations by total internal reflection fluorescence microscopy (Figure 3). Elongation rates were linearly proportional to the concentration of actin monomers up to 1.75 μM actin. The slope and intercept gave association and dissociation rate constants of 12.6 μM^{-1} s^{-1} and 0.09 s^{-1}, respectively, and a K_d of 0.01 μM^{-1}. The elongation rate was higher than expected at 2.5 μM actin. However, in addition to elongating existing filaments, AMP-PNP-actin monomers spontaneously formed many more short filaments than ATP-actin monomers (not shown), indicating that nucleation is

dx.doi.org/10.1021/bi400682n | Biochemistry 2013, 52, 6456−6466

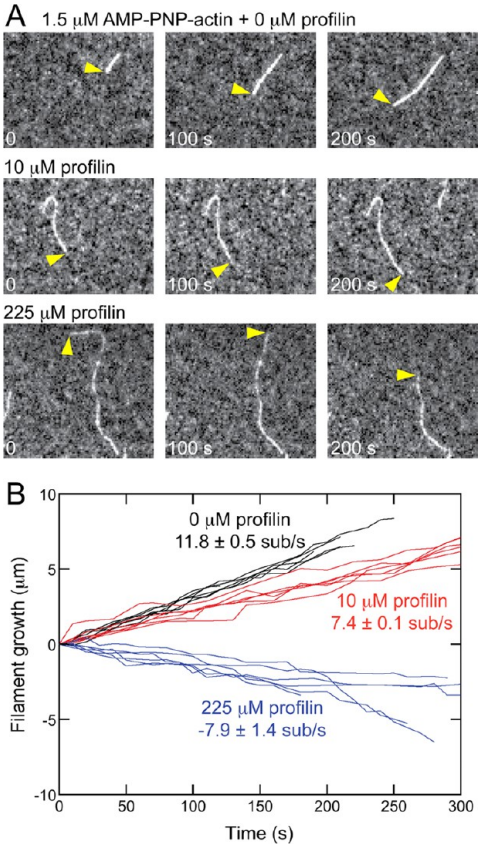

Figure 2. Effect of profilin on barbed end elongation of Mg-AMP-PNP-actin filaments. Polymerization conditions: 10 mM imidazole (pH 7.0), 50 mM KCl, 1 mM $MgCl_2$, 1 mM EGTA, 50 mM DTT, 0.37 mM AMP-PNP, 0.02 mM $CaCl_2$, 15 mM glucose, 0.02 mg/mL catalase, 0.1 mg/mL glucose oxidase, and 0.5% methylcellulose [4000 cP at 2% (w/v)]. Data were collected with total internal reflection fluorescence microscopy. (A) Time series of images of 1.5 μM AMP-PNP-actin (20% Alexa 488-labeled) filaments growing in the presence of a range of concentrations of human profilin 1. Yellow arrowheads denote barbed ends. (B) Time courses of the growth of six representative filament barbed ends in the presence of 1.5 μM AMP-PNP-actin (20% Alexa 488-labeled) and profilin concentrations of 0 (black), 10 (red), or 225 μM (blue).

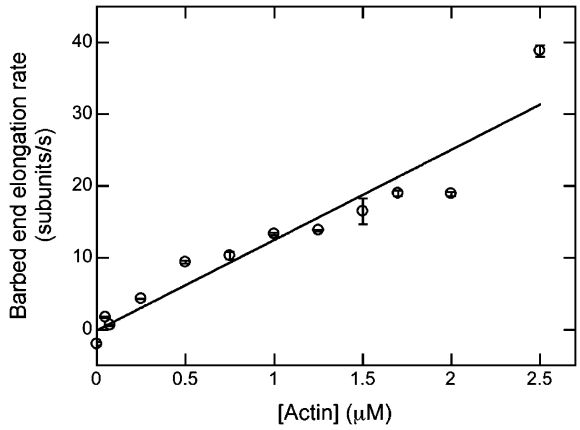

Figure 3. Dependence of the elongation rates of AMP-PNP-actin filaments on the concentration of AMP-PNP-actin monomers. Growth of filaments was observed by total internal reflection fluorescence microscopy with concentrations of AMP-PNP-actin (20% Alexa 488-labeled) from 50 nM to 2.5 μM in microscopy buffer with 0.37 mM AMP-PNP. Filament seeds were grown from 1.5 μM AMP-PNP-actin monomers in the observation chamber, followed by a wash and replacement with AMP-PNP-actin monomers. Error bars are one standard error of the mean elongation rate of at least 10 filaments.

much more favorable with AMP-PNP-actin than with ATP-actin. Annealing of the high concentration of short filaments with barbed ends may have contributed to the high elongation rate with 2.5 μM AMP-PNP-actin.

The rates of dissociation of actin subunits from filament ends in the absence of profilin were known for filaments polymerized from ATP-, ADP-P_i-, and ADP-actin monomers.[39,40] We determined the dissociation rate for AMP-PNP-actin by measuring the shortening of AMP-PNP-actin filaments after washing out the actin monomers with polymerization buffer alone (Table 1).

Effect of Profilin on Actin Filament Depolymerization in the Absence of Monomeric Actin. To obtain the rates of dissociation of profilin-actin from filament ends uncomplicated by association of profilin-actin with the ends, we measured shortening of filaments polymerized from ATP-, AMP-PNP-, ADP-P_i-, or ADP-actin monomers after washing out the actin monomers with polymerization buffer containing 750 μM human profilin but without free actin monomers (Table 1). Under these conditions, profilin should saturate the barbed ends, making profilin-actin the major species dissociating from the ends. As reported previously for ADP-actin,[15] a saturating level of profilin increased the rates that barbed ends shortened, with the most dramatic effect on Mg-AMP-PNP-actin filaments and the weakest effect on Mg-ADP-actin filaments (Table 1). Although the depolymerization rate we measured in saturating profilin for Mg-ADP-P_i-actin filaments (−8.6 subunits/s) was similar to that reported by Jegou and co-workers (−4.7 subunits/s),[20] the rate we observed using Mg-ADP-actin filaments (−12.2 subunits/s) was only 30% of that observed by Jegou and co-workers (−41 subunits/s). However, as discussed below, this range of depolymerization rates for Mg-ADP-actin does not affect our main conclusions.

Effect of Profilin on the Elongation and Shortening of Actin Filament Barbed Ends. To characterize the interactions of profilin with the barbed ends of filaments, we observed actin filament elongation or shortening at profilin concentrations ranging from 10 to 150 μM for 1.5 μM Mg-ATP-actin, from 5 to 225 μM for 1.5 μM AMP-PNP-actin, from 2.5 to 300 μM for 4 μM ADP-P_i-actin, and from 0.5 to 25 μM for 5 μM Mg-ADP-actin (Figure 4). Most filaments grew at steady rates throughout the observation times, interrupted in some cases by short, obvious pauses.

Profilin inhibited elongation of actin filament barbed ends in a concentration-dependent fashion. Stoichiometric concentrations of profilin stopped barbed end elongation with 5 μM ADP-actin (Figure 4D), whereas ~60 μM profilin was required to stop elongation in the presence of 1.5 μM ATP-actin (Figure 4A). Profilin concentrations higher than those required to stop elongation caused barbed ends to shorten, and short filaments eventually depolymerized and disappeared. A few barbed ends did not shorten immediately or paused for 45−60 s as they depolymerized. Encounters of depolymerizing barbed ends with myosin attachment points may have contributed to these pauses, because barbed ends fluctuated laterally much less during pauses than before and after these delays. Alternatively, laser-induced subunit cross-linking may also have contributed to some pauses.[41] Elongation rates fell on smooth curves at low and high profilin

dx.doi.org/10.1021/bi400682n | Biochemistry 2013, 52, 6456−6466

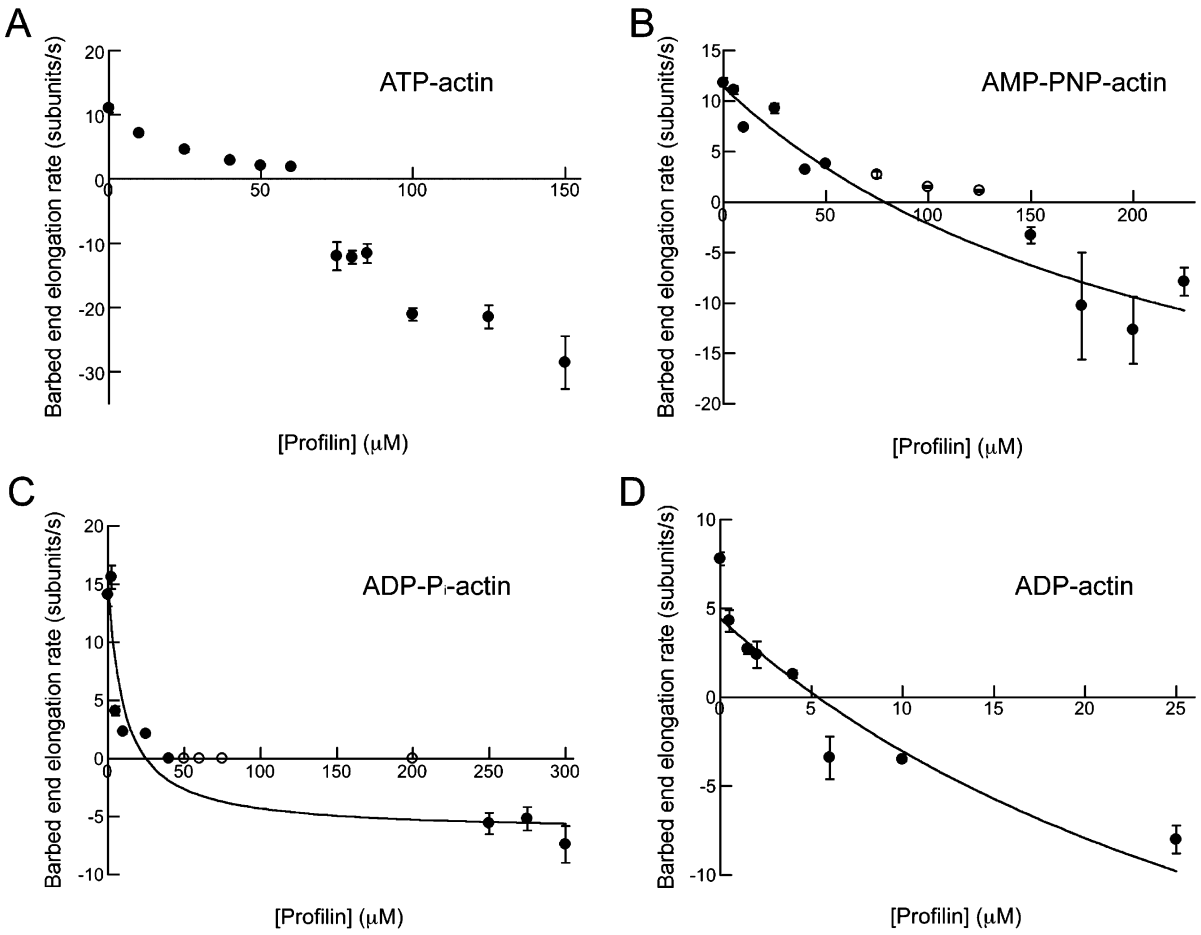

Figure 4. Dependence of barbed end elongation rates of Mg-ATP-, Mg-AMP-PNP-, Mg-ADP-P_i-, and Mg-ADP-actin monomers on the concentration of profilin 1. Data were collected by total internal reflection fluorescence microscopy. Error bars are standard errors of the mean elongation rates of at least 10 filaments. The smooth curves are fits to the filled data points with the model described in the text. Data shown as empty circles were masked in these fits. (A) Conditions for Mg-ATP-actin monomers: 1.5 μM ATP-actin (20% Alexa 488-labeled), 0.2 mM ATP, and a range of concentrations of profilin in microscopy buffer. (B) Conditions for Mg-AMP-PNP-actin monomers: 1.5 μM AMP-PNP-actin (20% Alexa 488-labeled), 0.37 mM AMP-PNP, and a range of concentrations of profilin in microscopy buffer. (C) Conditions for Mg-ADP-P_i-actin monomers: 4 μM Mg-ADP-P_i-actin (20% Alexa 488-labeled), 0.3 mM ADP, 20 units/mL hexokinase, 12.5 mM potassium phosphate, and a range of concentrations of profilin in microscopy buffer. The polymerization buffer contained 25 mM KCl instead of 50 mM KCl to compensate for the additional K^+ ions. (D) Conditions for Mg-ADP-actin monomers: 5.0 μM Mg-ADP-actin (20% Alexa 488-labeled), 0.3 mM ADP, 20 units/mL hexokinase, and a range of concentrations of profilin in microscopy buffer.

concentrations but not at intermediate profilin concentrations (40−60 μM profilin for ATP-actin, 75−125 μM profilin for AMP-PNP-actin, and 50−75 μM profilin for ADP-P_i-actin) where elongation rates were near zero [Figure 4A−C (○)]. Long time scales were required to visualize these low rates of polymerization and depolymerization, so photo-cross-linking events may have compromised the measurements. For this reason, we did not include these intermediate data points in our analysis (see below).

Effect of Profilin on the Elongation of Actin Filament Barbed Ends by AMP-PNP-Actin. Barbed end elongation rates with 1.5 μM Mg-AMP-PNP-actin monomers were close to zero with ∼100 μM profilin (Figure 4B), 20-fold higher than the concentration required to stop elongation of barbed ends by Mg-ADP-actin monomers (Figure 4D). Profilin concentrations of >125 μM caused barbed ends to shorten. Given the low concentration of total AMP-PNP-actin monomers (1.5 μM) and their high affinity for profilin (K_{d1} = 0.1 μM), most AMP-PNP-actin monomers were bound to profilin at all profilin concentrations (5−225 μM) tested, so the main species that varied with total profilin concentration was the free profilin concentration. The experimental data in Figure 4B revealed that this free profilin was titrating a species with a very low affinity for barbed ends.

We fit our polymerization data using eq 4 and extracted the affinities of profilin and profilin-AMP-PNP-actin for AMP-PNP-actin filament barbed ends using the association and dissociation rates summarized in Table 2. The results of our fitting indicate that the affinity of AMP-PNP-actin filament barbed ends for the profilin-AMP-PNP-actin complex (K_d = 4.6 μM) is 49-fold higher than for free profilin (K_d = 226 μM). The data strongly constrain the ratio of these two equilibrium constants, as demonstrated by a plot of the R^2 value of fits performed by fixing K_{d3} at 226 μM and varying the value of K_{d4} (Figure S1A of the Supporting Information). Although a range of values of K_{d3} and K_{d4} fit the data reasonably well as long as their ratio remains the same, the particular combination of 226 and 4.6 μM provides the best fit to our data (not shown). Thus, association of the profilin-AMP-PNP-actin complex is the main pathway capping barbed ends and inhibiting elongation. Second, because profilin-AMP-PNP-actin and monomeric AMP-PNP-actin bind to barbed ends at similar rates, the large difference in their affinities arises from much faster

dx.doi.org/10.1021/bi400682n | *Biochemistry* 2013, 52, 6456−6466

Table 2. Summary of Reaction Rates and Affinities for AMP-PNP-, ADP-P_i-, and ADP-Actin and Profilin

	reaction	AMP-PNP				ADP-P_i				ADP			
		k_- (s^{-1})	k_- (s^{-1})	K_d (μM)	ΔG (kcal/mol)	k_+ (μM^{-1} s^{-1})	k_+ (μM^{-1} s^{-1})	K_d (μM)	ΔG (kcal/mol)	k_+ (μM^{-1} s^{-1})	k_- (s^{-1})	K_d (μM)	ΔG (kcal/mol)
1	A + P ⇆ PA	14[d]	1.3[d]	0.1[d]	9.5	14[d]	1.3[d]	0.1[d]	9.5	15.6[d]	2.6[d]	0.2[d]	9.1
2	A + BE ⇆ BE + F	12.6[a]	0.09[a]	0.01[a]	10.9	3.4[e]	0.2[e]	0.06[e]	9.8	2.9[e]	5.0[e]	1.7[e]	7.9
3	BE + P ⇆ BE−P	nd[c]	n.d.[c]	226[b]	5.0	nd[c]	nd[c]	10.2[b]	6.8	nd[c]	nd[c]	0.9[b]	8.2
4	PA + BE ⇆ BE−P + F	11.4[b]	52.4[a]	4.6[b]	7.3	4.1[b]	8.6[a]	2.1[b]	7.7	0.3[b]	12.2[a]	36.7[b]	6.0

[a]Rates and affinities measured in this study. [b]Rates and affinities extracted from our fitting analysis. [c]Not determined. [d]See ref 36. We assumed similar thermodynamics for binding of profilin to ATP-actin, AMP-PNP-actin, and ADP-P_i-actin monomers. [e]See ref 39.

dissociation of profilin-AMP-PNP-actin from barbed ends (which we measured directly). Free energy calculations for each of the binding reactions reveal that the thermodynamic parameters produced by our fitting are balanced [within 0.9 kcal/mol (Figure 1)], and therefore, these four reactions are sufficient to describe the polymerization of AMP-PNP-actin in the presence of profilin.

Effect of Profilin on the Elongation of Actin Filament Barbed Ends by ADP-P_i-Actin. Barbed end elongation rates with 4 μM Mg-ADP-P_i-actin monomers were zero with ~40 μM profilin (Figure 4C), ~2.5-fold lower than the profilin concentration required to stop elongation of barbed ends by Mg-AMP-PNP-actin monomers. Profilin concentrations ranging from 40 to 200 μM appeared to stall polymerization, perhaps because of photo-cross-linking events that accumulate during the long times required to visualize and measure small depolymerization rates. However, profilin concentrations of >225 μM caused barbed ends to shorten. Given the high affinity of ADP-P_i-actin for profilin (K_{d1} = 0.1 μM), most of the ADP-P_i-actin monomers were bound to profilin at all profilin concentrations (2.5−300 μM) tested, so the main species that varied with total profilin concentration was the free profilin concentration.

Using eq 4 to fit the ADP-P_i-actin polymerization data, we determined that the affinity of ADP-P_i-actin filament barbed ends is 5-fold higher for the profilin-ADP-P_i-actin complex than for free profilin. As with our AMP-PNP-actin data, the ADP-P_i-actin polymerization data strongly constrain the ratio of these two equilibrium constants, as demonstrated by a plot of the R^2 value of fits performed by fixing K_{d3} at 10.2 μM and varying the value of K_{d4} (Figure S1B of the Supporting Information). Although a range of values of K_{d3} and K_{d4} fit the data reasonably well as long as their ratio remains the same, the particular combination of 10.2 and 2.1 μM provides the best fit to our data (not shown). Thus, both direct binding of profilin and association of profilin-ADP-P_i-actin contribute to capping barbed ends. Second, as we observed for AMP-PNP-actin, the association rate constants for monomeric ADP-P_i-actin and profilin-bound ADP-P_i-actin with barbed ends are similar, so the dissociation rate constants determine the affinities. Free energy calculations show that our thermodynamic parameters are balanced (within 0.6 kcal/mol) for the reactions involving ADP-P_i-actin (Figure 1).

Effect of Profilin on the Elongation of Actin Filament Barbed Ends by ADP-Actin. Low micromolar profilin concentrations inhibited elongation of barbed ends by 5 μM Mg-ADP-actin monomers, whereas profilin concentrations exceeding 5 μM depolymerized barbed ends (Figure 4C). Unconstrained fits to our elongation data produced negative dissociation equilibrium constants for reaction 3 (K_{d3}). To correct this problem, we varied the difference between K_{d2} and K_{d4} over a range of larger values until fitting yielded positive dissociation equilibrium constants for all reactions. The goodness of the fit decreased as the difference between K_{d2} and K_{d4} increased, so our final fit represents both the best fit to the data with positive dissociation equilibrium constants for all reactions and a lower limit for the value of K_{d4}. The low affinity of profilin-ADP-actin for barbed ends results from slow association of profilin-ADP-actin with barbed ends. The upper limit of the association rate constant is 10-fold lower than that for binding of free ADP-actin to barbed ends.

The interactions of ADP-actin with profilin differ qualitatively from those of AMP-PNP-actin and ADP-P_i-actin. The affinity of free profilin for ADP-actin barbed ends is 40-fold greater than the affinity of profilin-ADP-actin for barbed ends,

dx.doi.org/10.1021/bi400682n | Biochemistry 2013, 52, 6456−6466

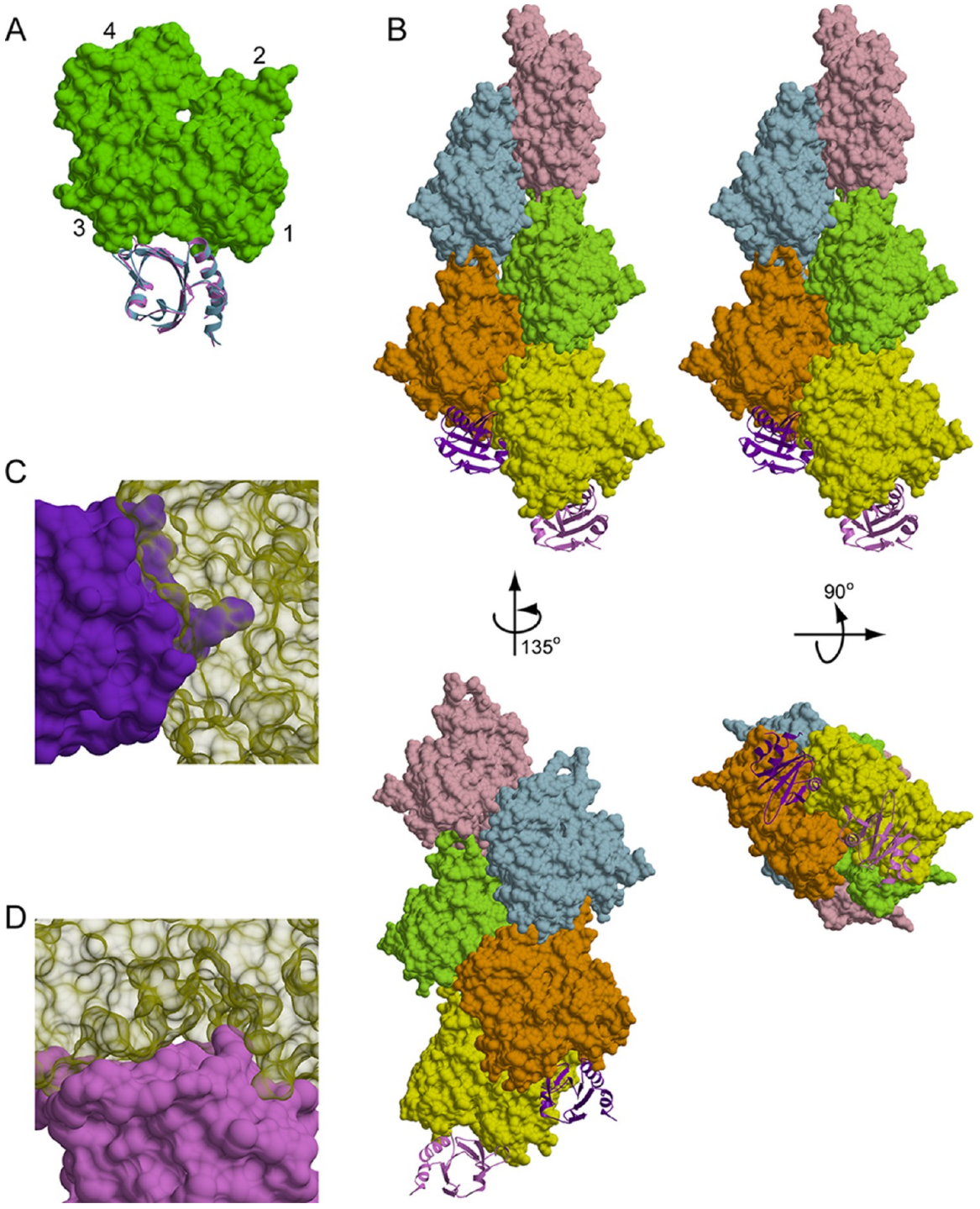

Figure 5. Molecular models showing steric clashes produced by binding of profilin to the terminal subunits of both long-pitch helices (subunits *n* and *n* − 1) of an actin filament. A solvent-excluded surface model of actin and ribbon diagrams of profilin are shown. (A) Superposition of human profilin (purple, PDB entry 1FIK) onto the structure of bovine *β*-actin (green) bound with bovine profilin (blue, PDBD entry 1HLU). (B) Stereoview (top) of an Oda actin filament model[30] with human profilin 1 (dark purple and light purple) bound to the terminal subunits of each long-pitch helix (subunits *n* and *n* − 1) as in panel A. Additional views (bottom) of the filament and bound profilin molecules. (C) Detail of the clashes formed between profilin (dark purple) and subdomain 1 of actin subunit *n* (yellow) when profilin is bound to actin subunit *n* − 1. Solvent-excluded surfaces are shown.[33] (D) Detail of the profilin-actin interface at the terminal barbed end subunit (profilin, light purple; actin subunit *n*, yellow). Solvent-excluded surfaces are shown.[33]

while the opposite is true for the interaction of profilin with AMP-PNP-actin or ADP-P_i-actin monomers and barbed ends. This is reflected in the lower limit for the dissociation equilibrium constant of profilin-ADP-actin on barbed ends (K_{d4}), which represents an affinity approximately 8-fold lower than that for profilin-AMP-PNP-actin and 20-fold lower than that for ADP-P_i-actin binding to barbed ends.

Our analysis yielded an affinity of profilin for ADP-actin barbed ends (K_{d3} = 0.9 μM) higher than that reported by Jegou and co-workers[20] (K_{d3} = 28.1 μM). This group obtained their

dx.doi.org/10.1021/bi400682n | *Biochemistry* 2013, 52, 6456−6466

binding constant by fitting a hyperbolic curve to the dependence of the rates of depolymerization of filaments assembled from Mg-ADP-actin on the concentrations of profilin without actin monomers. However, profilin-stimulated filament depolymerization involves two sequential reactions: binding of profilin to the barbed end followed by dissociation of profilin-actin from the barbed end. Thus, the binding constant obtained from their fitting does not correspond to one reaction. Instead, their fitting parameter is a combination of binding constants for profilin on barbed ends (K_{d3} = 0.9 μM in our work) and profilin-actin on barbed ends (K_{d4} = 36.7 μM in our work). In a separate study, Kinosian et al.[15] assumed that profilin binds ADP-actin monomers and barbed ends with the same association rate constant of 15 μM^{-1} s^{-1}. Although our data analysis does not produce an association rate constant for binding of profilin to barbed ends, their assumption led them to estimate a K_d of 20 μM for binding of profilin-actin to barbed ends, which is similar to our measurement.

We observed a slower depolymerization rate for ADP-actin with saturating profilin than Jegou and co-workers did.[20] However, we agree with them that the rate of depolymerization of filaments assembled from ATP-actin increases over time in the presence of high concentrations of profilin (Figure S2 of the Supporting Information). The fastest dissociation rate in our experiment (−32 subunits/s in 125 μM profilin) approached the rate of −41 subunits/s observed by Jegou and co-workers for ADP-actin depolymerization in 80 μM profilin. As they suggested, this rate might correspond to the depolymerization of ADP-actin subunits that had hydrolyzed and dissociated phosphate. The differing affinities of profilin for barbed ends polymerized from AMP-PNP-, ADP-P_i-, and ADP-actin suggest that filaments with each type of bound nucleotide have novel conformations (see below). It is also possible that nucleotide heterogeneity of the ends of aging filaments polymerized from ATP-actin might make them less stable than homogeneous ADP-P_i- or ADP-actin filament ends.

We draw the same conclusions from our thermodynamic analysis about the affinities of profilin and profilin-actin for barbed ends if we use our value of −12 subunits/s or Jegou's value of −41 subunits/s for the rate of dissociation of profilin-ADP-actin from barbed ends. If we use an actin dissociation rate in 750 μM profilin of −41 subunits/s with our other data on ADP-actin (Figure 3C), the best fit gives a K_{d3} of 14.4 μM and a K_{d4} of 68.5 μM (not shown). This affinity (K_{d4}) of profilin-ADP-actin monomers for barbed ends is weaker by a factor of only 2 compared with that from the fit to our data. Similarly, calculation of the association rate constant for binding of profilin-ADP-actin to barbed ends (k_4^+) produces a rate constant of 0.8 μM^{-1} s^{-1}, which is similar to the rate constant of 0.3 μM^{-1} s^{-1} we obtained using our data and is still slower than that for binding of free ADP-actin monomers to barbed ends. Including the faster profilin-actin dissociation rate in the analysis reduces the calculated affinity of profilin for ADP-bound barbed ends 15-fold. However, this lower affinity is still tighter than the affinity of profilin-ADP-actin monomers for barbed ends and does not affect our conclusions or the structural implications of our results (see below), given that it is on the same order of magnitude as the calculated affinity of profilin for ADP-P_i-actin for barbed ends.

We conclude that profilin slows the elongation of filaments by ADP-actin through three mechanisms. First, profilin binds barbed ends with relatively high affinity ($K_{d3} \sim 1$ μM) where it blocks the association of actin monomers and profilin-actin. Second, profilin bound to a barbed end dissociates along with the terminal subunit at least twice as fast as an ADP-actin subunit alone. In addition, ADP-actin bound to profilin associates with barbed ends much slower than free ADP-actin. The thermodynamics of the system are within 1 kcal/mol of detailed balance (Figure 1). However, as noted above, our fitting represents a lower limit for K_{d3} (the affinity of profilin for the barbed end). Fitting the data with a larger K_{d3} for the binding of profilin to the barbed end brings the system closer to equilibrium. For example, using a K_{d3} of 5.2 μM results in a slightly weaker affinity of profilin-actin for barbed ends (K_{d4} = 50 μM) and brings the system within 0.1 kcal/mol of detailed balance.

Structural Analysis. We used molecular models to determine if profilin might bind to either or both the terminal and penultimate subunits at the barbed end of a filament. We used the cocrystal structure of an actin monomer and bovine profilin[8] to dock human profilin on the two terminal subunits at the barbed end of an Oda[30] actin filament model (Figure 5). Because polymerized actin has a slightly flatter conformation than an actin monomer, profilin clashes directly with the subunit to which it is bound (Figure 5D). Specifically, we measured a total of 11 steric clashes (which we defined as contacts of <2.2 Å) involving atoms from five profilin residues (residues 59, 60, and 72−74) and five residues in actin subdomains 1 and 3 (residues 171, 173, 284, 286, and 375). Furthermore, profilin bound to the penultimate (n − 1) subunit clashes with residues 223−228 and 259−272 in subdomain 4 of actin subunit n. Similar models showed that both *Schizosaccharomyces pombe* profilin and *Saccharomyces cerevisiae* profilin have similar clashes with adjacent subunits.

This analysis shows that profilin can bind only the barbed end of terminal subunit n and that profilin bound to this site precludes the addition of an actin subunit to either the terminal or penultimate subunit. To avoid steric clashes with the bound profilin, the conformation of this terminal subunit must be slightly less flat than the rest of the subunits in the filament. Profilin can come to be bound to the terminal subunit on the barbed end of a filament either by binding directly or by binding as a profilin-actin complex. Profilin bound to the terminal subunit on the barbed end of a filament can either dissociate directly from this subunit or dissociate along with the terminal actin subunit as a profilin-actin complex.[9]

DISCUSSION

We undertook a thermodynamic analysis to determine rate and equilibrium constants for the various reactions involved in actin filament polymerization in the presence of profilin. Technical limitations had prevented direct measurement of these parameters in previous studies, but single-filament visualization allowed us to measure elongation and shortening rates in the presence of a range of concentrations of profilin. Fitting a thermodynamic model to the profilin concentration dependence of these elongation rates yielded equilibrium constants and several rate constants for binding of profilin and profilin-actin to filament barbed ends. We found that although profilin has a higher affinity for ATP-actin monomers than ADP-actin monomers, it has a much higher affinity for the barbed ends of ADP-actin filaments than ATP-actin filaments or AMP-PNP-actin filaments. In addition, binding of profilin to monomers has a 20-fold stronger effect on binding of the AMP-PNP-actin monomer to filament barbed ends than for ADP-actin monomers and filaments.

Structural Implications of Our Data Analysis. The differences in the affinities of AMP-PNP- and ADP-bound

dx.doi.org/10.1021/bi400682n | *Biochemistry* 2013, 52, 6456−6466

barbed ends for profilin and profilin-actin strongly suggest that barbed end subunits have conformations different from those of monomers and that these conformations change upon nucleotide hydrolysis and phosphate release. Although experimental evidence of conformational dynamics of filamentous actin subunits in living cells is not available, we propose answers to three fundamental questions about these interactions on the basis of our work with purified proteins.

Why Does Profilin Have a Higher Affinity for Actin Monomers Than for Barbed Ends? Regardless of the nucleotide bound to actin, profilin has a higher affinity for actin monomers than for actin filament barbed ends. The most likely explanation is that ADP-actin subunits in filaments have subdomains 3 and 4 rotated relative to subdomains 1 and 2, resulting in flattening of the subunit relative to the monomer.[30,42] This rotation in the filament alters the orientation of the two halves of the profilin binding site located on the "bottoms" of subdomains 1 and 3 flanking the barbed end groove,[8] creating minor steric clashes that can explain the lower affinity of profilin for barbed ends (Figure 5).

Thus, to bind profilin, the actin subunit at the barbed end of an actin filament must take up at least transiently a conformation different from the average internal subunit. Conformational changes to accommodate profilin binding are most likely to occur within the terminal actin, because profilin is not known to populate different conformations. The well-documented structural heterogeneity among the subunits of polymerized actin[43] suggests that they possess inherent flexibility that may contribute to profilin binding.

How Does the Bound Nucleotide Influence the Affinity of Profilin for Barbed Ends? The nucleotide bound to actin monomers has only a small influence on the affinity for profilin compared with the large impact of the bound nucleotide on the affinity of barbed ends for profilin. The affinities of ADP-actin monomers and barbed ends differ by only 4.5-fold, while profilin binds much more weakly to barbed ends than monomers of AMP-PNP-actin (2260-fold) and ADP-P_i-actin (102-fold). These huge differences in affinities suggest that the structures of the subunits at the barbed end of ADP-actin filaments may resemble actin monomers more closely than the terminal subunits of AMP-PNP-actin and ADP-P_i-actin filaments. We suggest that the absence of the γ-phosphate allows a terminal ADP-actin subunit greater freedom to assume monomer-like conformations that are favorable for binding profilin. Structures of barbed ends with different nucleotides (comparable to the cryoelectron microscopy structure of pointed ends[44]) should be very informative.

Why Do Barbed Ends Have a Higher Affinity for Actin Monomers Than for Profilin-Actin? Bound profilin weakens the affinity of actin subunits for barbed ends. Although the nucleotide binding cleft may be open or closed in crystal structures of actin monomers bound to profilin,[8,45,46] none of these structures has subdomains 3 and 4 rotated relative to subdomains 1 and 2 as observed in filaments.[30,42] This suggests that bound profilin may limit the conformational flexibility of actin monomers and reduce their ability to undergo the conformational changes associated with polymerization. For all three nucleotide states, bound profilin increases the dissociation rate constant of the terminal subunit, suggesting that profilin bound to the terminal subunit favors a conformation that compromises interfacial contacts with subunits $n - 1$ and $n - 2$.

The difference in the affinity of barbed ends for actin monomers and profilin-actin is much greater for AMP-PNP-actin than for ADP-P_i-actin and ADP-actin. This suggests that nucleotide hydrolysis and subsequent phosphate release alleviate some of the effects of profilin binding on the actin subunit conformational flexibility. However, because of the low affinity of barbed ends for P_i,[39] it is likely that some of the ADP-P_i-actin barbed ends observed in our experiments are really ADP-actin barbed ends. This makes it difficult to quantify the relative effects of nucleotide hydrolysis and phosphate release on barbed end affinity.

Profilin bound to ADP-actin monomers also slows their association with barbed ends. Even though the profilin-binding sites of ADP-actin monomers and barbed ends resemble each other, it follows from detailed balance that the relatively tightly bound profilin will compromise association of monomeric ADP-actin with barbed ends. This may be achieved via an allosteric effect on subunits 1 and 2, which associate with the barbed end and have been demonstrated to populate a variety of conformational modes in filaments.[43]

Effect of Profilin on the Elongation of Actin Filament Barbed Ends by ATP-Actin. Barbed end elongation rates with 1.5 μM Mg-ATP-actin monomers were close to zero with ~60 μM profilin (Figure 4A), a profilin concentration between the concentrations required to stop elongation of barbed ends by Mg-AMP-PNP- and Mg-ADP-P_i-actin monomers (Figure 4B,C). Profilin concentrations of >75 μM caused barbed ends to shorten in the presence of Mg-ATP-actin monomers. Given the low concentration of total ATP-actin (1.5 μM) and its high affinity for profilin (K_{d1} = 0.1 μM), most ATP-actin monomers were bound to profilin at all profilin concentrations (10−150 μM) tested, so the main species that varied with total profilin concentration was the free profilin concentration. Because of the heterogeneity in the nucleotide composition of the filaments, we did not perform a thermodynamic analysis of the elongation data. However, we estimate that the free profilin titrated a species with an affinity for barbed ends that lies in the range of 10−226 μM (or between the affinity of profilin for barbed ends composed of Mg-ADP-P_i-actin and Mg-AMP-PNP-actin). Further, because filaments elongated in the presence of profilin concentrations where all of the actin was likely to be bound to profilin (10−60 μM total profilin), Mg-ATP-actin-profilin complexes must have a higher affinity for barbed ends than free profilin. We estimate this affinity to be in the low micromolar range, as observed for Mg-ADP-P_i-actin and Mg-AMP-PNP-actin.

The energetics of filament elongation in the presence of profilin have puzzled the field since it was discovered that actin monomers saturated with profilin can elongate barbed ends.[9] Investigators proposed that binding reactions provide the energy for polymerization of ATP-actin[15,18] or that energy from ATP hydrolysis is required to balance the reaction.[47] However, because the thermodynamic parameters we obtain from our data analysis are balanced for AMP-PNP-actin, ADP-P_i-actin, and ADP-actin monomers, we hypothesize that the four reactions described above are balanced during ATP-actin polymerization with profilin, regardless of the age (and therefore nucleotide state) of the subunits at the barbed end, and that no additional energy is required for polymerization.

Implications for Profilin Function *in Vivo*. Our results fill in several missing kinetic and thermodynamic parameters that are required to explain how profilin influences actin polymerization in cells. At cellular profilin concentrations in the range of 100 μM, most unpolymerized actin is bound to profilin[13] and little free profilin is available to bind barbed ends. The high concentration of profilin-actin adds to free barbed ends and also promotes elongation of barbed ends associated with a formin

by binding to the FH1 domain and being delivered rapidly to the end of the filament.[28,48] If a filament is severed, exposing a barbed end with terminal ADP-actin subunits, free profilin might bind and promote dissociation of subunits at a rate (12 s^{-1}) faster than the rate of dissociation of ADP-actin from a free end. However, given ~100 μM profilin-ATP-actin in the cytoplasm,[13] the filament will grow until it is capped. In cells with thymosin-β4, that protein sequesters part of the unpolymerized actin,[47,49] adding another factor to consider.

■ ASSOCIATED CONTENT

Supporting Information

Reaction rates and affinities for ATP-actin and profilin (Table S1), the dependence of R^2 values of fits obtained from our data analysis on the absolute value of K_{d4} for AMP-PNP-actin and ADP-P_i-actin (Figure S1), and depolymerization of representative ATP-actin filament barbed ends in the presence of profilin (Figure S2). This material is available free of charge via the Internet at http://pubs.acs.org.

■ AUTHOR INFORMATION

Corresponding Author

*E-mail: thomas.pollard@yale.edu. Phone: (203) 432-3565.

Funding

This work was supported by National Institutes of Health Grant GM-026338 and a postdoctoral fellowship from the Leukemia and Lymphoma Society.

Notes

The authors declare no competing financial interest.

■ ACKNOWLEDGMENTS

We thank Aaron G. Downs for conducting preliminary experiments, Christopher Jurgenson and Mark Zweifel for help with molecular graphics, and Julien Berro for help with the thermodynamic analysis.

■ REFERENCES

(1) Birbach, A. (2008) Profilin, a multi-modal regulator of neuronal plasticity. *BioEssays 30*, 994−1002.

(2) Carlsson, L., Nyström, L. E., Sundkvist, I., Markey, F., and Lindberg, U. (1977) Actin polymerizability is influenced by profilin, a low molecular weight protein in non-muscle cells. *J. Mol. Biol. 115*, 465−483.

(3) Markey, F., Larsson, H., Weber, K., and Lindberg, U. (1982) Nucleation of actin polymerization from profilactin opposite effects of different nuclei. *Biochim. Biophys. Acta 704*, 43−51.

(4) Tseng, P. C., and Pollard, T. D. (1982) Mechanism of action of *Acanthamoeba* profilin: Demonstration of actin species specificity and regulation by micromolar concentrations of $MgCl_2$. *J. Cell Biol. 94*, 213−218.

(5) Tobacman, L. S., Brenner, S. L., and Korn, E. D. (1983) Effect of *Acanthamoeba* profilin on the pre-steady state kinetics of actin polymerization and on the oncentration of F-actin at steady state. *J. Biol. Chem. 258*, 8806−8812.

(6) Pollard, T. D., and Cooper, J. A. (1984) Quantitative analysis of the effect of *Acanthamoeba* profilin on actin filament nucleation and elongation. *Biochemistry 23*, 6631−6641.

(7) Vandekerckhove, J., Kaiser, D. A., and Pollard, T. D. (1989) *Acanthamoeba* actin and profilin can be crosslinked between glutamic acid 364 of actin and lysine 115 of profilin. *J. Cell Biol. 109*, 619−626.

(8) Schutt, C. E., Myslik, J. C., Rozycki, M. D., Goonesekere, N. C., and Lindberg, U. (1993) The structure of crystalline profilin-β-actin. *Nature 365*, 810−816.

(9) Yarmola, E. G., and Bubb, M. R. (2009) How depolymerization can promote polymerization: The case of actin and profilin. *BioEssays 31*, 1150−1160.

(10) Tilney, L. G., Bonder, E. M., Coluccio, L. M., and Mooseker, M. S. (1983) Actin from *Thyone briareus* sperm assembles on only 1 end of an actin filament: A behavior regulated by profilin. *J. Cell Biol. 97*, 112−142.

(11) Hill, T. L. (1983) Length dependence of rate constants for end-to-end association and dissociation of equilibrium linear aggregates. *Biophys. J. 44*, 285−288.

(12) Gutsche-Perelroizen, I., Lepault, J., Ott, A., and Carlier, M. F. (1999) Filament assembly from profilin-actin. *J. Biol. Chem. 274*, 6234−6243.

(13) Kaiser, D. A., Vinson, V. K., Murphy, D. B., and Pollard, T. D. (1999) Profilin is predominantly associated with monomeric actin in *Acanthamoeba*. *J. Cell Sci. 112* (Part 21), 3779−3790.

(14) Kang, F., Purich, D. L., and Southwick, F. S. (1999) Profilin promotes barbed-end actin filament assembly without lowering the critical concentration. *J. Biol. Chem. 274*, 36963−36972.

(15) Kinosian, H. J., Selden, L. A., Gershman, L. C., and Estes, J. E. (2002) Actin filament barbed end elongation with nonmuscle MgATP-actin and MgADP-actin in the presence of profilin. *Biochemistry 41*, 6734−6743.

(16) Kinosian, H. J., Selden, L. A., Gershman, L. C., and Estes, J. E. (2004) Non-muscle actin filament elongation from complexes of profilin with nucleotide-free actin and divalent cation-free ATP-actin. *Biochemistry 43*, 6253−6260.

(17) Lal, A. A., and Korn, E. D. (1985) Reinvestigation of the inhibition of actin polymerization by profilin. *J. Biol. Chem. 260*, 10132−10138.

(18) Pring, M., Weber, A., and Bubb, M. R. (1992) Profilin-actin complexes directly elongate actin filaments at the barbed end. *Biochemistry 31*, 1827−1836.

(19) Bubb, M. R., Yarmola, E. G., Gibson, B. G., and Southwick, F. S. (2003) Depolymerization of actin filaments by profilin. Effects of profilin on capping protein function. *J. Biol. Chem. 278*, 24629−24635.

(20) Jegou, A., Niedermayer, T., Orban, J., Didry, D., Lipowsky, R., Carlier, M. F., and Romet-Lemonne, G. (2011) Individual actin filaments in a microfluidic flow reveal the mechanism of ATP hydrolysis and give insight into the properties of profilin. *PLoS Biol. 9*, e1001161.

(21) MacLean-Fletcher, S., and Pollard, T. D. (1980) Identification of a factor in conventional muscle actin preparations which inhibits actin filament self-association. *Biochem. Biophys. Res. Commun. 96*, 18−27.

(22) Houk, T. W., Jr., and Ue, K. (1974) The measurement of actin concentration in solution: A comparison of methods. *Anal. Biochem. 62*, 66−74.

(23) Kellogg, D. R., Mitchison, T. J., and Alberts, B. M. (1988) Behaviour of microtubules and actin filaments in living *Drosophila* embryos. *Development 103*, 675−686.

(24) Pollard, T. D. (1984) Polymerization of ADP-actin. *J. Cell Biol. 99*, 769−777.

(25) Fedorov, A. A., Pollard, T. D., and Almo, S. C. (1994) Purification, characterization and crystallization of human platelet profilin expressed in *Escherichia coli*. *J. Mol. Biol. 241*, 480−482.

(26) Kaiser, D. A., Goldschmidt-Clermont, P. J., Levine, B. A., and Pollard, T. D. (1989) Characterization of renatured profilin purified by urea elution from poly-L-proline agarose columns. *Cell Motil. Cytoskeleton 14*, 251−262.

(27) Lu, J., and Pollard, T. D. (2001) Profilin binding to poly-L-proline and actin monomers along with ability to catalyze actin nucleotide exchange is required for viability of fission yeast. *Mol. Biol. Cell 12*, 1161−1175.

(28) Paul, A. S., and Pollard, T. D. (2008) The role of the FH1 domain and profilin in formin-mediated actin-filament elongation and nucleation. *Curr. Biol. 18*, 9−19.

(29) Kuhn, J. R., and Pollard, T. D. (2005) Real-time measurements of actin filament polymerization by total internal reflection fluorescence microscopy. *Biophys. J. 88*, 1387−1402.
(30) Oda, T., Iwasa, M., Aihara, T., Maeda, Y., and Narita, A. (2009) The nature of the globular- to fibrous-actin transition. *Nature 457*, 441−445.
(31) Krissinel, E., and Henrick, K. (2004) Secondary-structure matching (SSM), a new tool for fast protein structure alignment in three dimensions. *Acta Crystallogr. D60*, 2256−2268.
(32) Winn, M. D., Ballard, C. C., Cowtan, K. D., Dodson, E. J., Emsley, P., Evans, P. R., Keegan, R. M., Krissinel, E. B., Leslie, A. G., McCoy, A., McNicholas, S. J., Murshudov, G. N., Pannu, N. S., Potterton, E. A., Powell, H. R., Read, R. J., Vagin, A., and Wilson, K. S. (2011) Overview of the CCP4 suite and current developments. *Acta Crystallogr. D67*, 235−242.
(33) Sanner, M. F., Olson, A. J., and Spehner, J. C. (1996) Reduced surface: An efficient way to compute molecular surfaces. *Biopolymers 38*, 305−320.
(34) Kraulis, P. J. (1991) MOLSCRIPT: A program to produce both detailed and schematic plots of protein structures. *J. Appl. Crystallogr. 24*, 946−950.
(35) Merritt, E. A., and Bacon, D. J. (1997) Raster3D: Photorealistic molecular graphics. *Methods Enzymol. 277*, 505−524.
(36) Kinosian, H. J., Selden, L. A., Gershman, L. C., and Estes, J. E. (2000) Interdependence of profilin, cation, and nucleotide binding to vertebrate non-muscle actin. *Biochemistry 39*, 13176−13188.
(37) Vinson, V. K., De La Cruz, E. M., Higgs, H. N., and Pollard, T. D. (1998) Interactions of *Acanthamoeba* profilin with actin and nucleotides bound to actin. *Biochemistry 37*, 10871−10880.
(38) Amann, K. J., and Pollard, T. D. (2001) Direct real-time observation of actin filament branching mediated by Arp2/3 complex using total internal reflection fluorescence microscopy. *Proc. Natl. Acad. Sci. U.S.A. 98*, 15009−15013.
(39) Fujiwara, I., Vavylonis, D., and Pollard, T. D. (2007) Polymerization kinetics of ADP- and ADP-P_i-actin determined by fluorescence microscopy. *Proc. Natl. Acad. Sci. U.S.A. 104*, 8827−8832.
(40) Pollard, T. D. (1986) Rate constants for the reactions of ATP- and ADP-actin with the ends of actin filaments. *J. Cell Biol. 103*, 2747−2754.
(41) Niedermayer, T., Jegou, A., Chieze, L., Guichard, B., Helfer, E., Romet-Lemonne, G., Carlier, M. F., and Lipowsky, R. (2012) Intermittent depolymerization of actin filaments is caused by photo-induced dimerization of actin protomers. *Proc. Natl. Acad. Sci. U.S.A. 109*, 10769−10774.
(42) Fujii, T., Iwane, A. H., Yanagida, T., and Namba, K. (2010) Direct visualization of secondary structures of F-actin by electron cryomicroscopy. *Nature 467*, 724−728.
(43) Galkin, V. E., Orlova, A., Schroder, G. F., and Egelman, E. H. (2010) Structural polymorphism in F-actin. *Nat. Struct. Mol. Biol. 17*, 1318−1323.
(44) Narita, A., Oda, T., and Maeda, Y. (2011) Structural basis for the slow dynamics of the actin filament pointed end. *EMBO J. 30*, 1230−1237.
(45) Chik, J. K., Lindberg, U., and Schutt, C. E. (1996) The structure of an open state of β-actin at 2.65 Å resolution. *J. Mol. Biol. 263*, 607−623.
(46) Ferron, F., Rebowski, G., Lee, S. H., and Dominguez, R. (2007) Structural basis for the recruitment of profilin-actin complexes during filament elongation by Ena/VASP. *EMBO J. 26*, 4597−4606.
(47) Pantaloni, D., and Carlier, M. F. (1993) How profilin promotes actin filament assembly in the presence of thymosin β4. *Cell 75*, 1007−1014.
(48) Kovar, D. R., Harris, E. S., Mahaffy, R., Higgs, H. N., and Pollard, T. D. (2006) Control of the assembly of ATP- and ADP-actin by formins and profilin. *Cell 124*, 423−435.
(49) Cassimeris, L., Safer, D., Nachmias, V. T., and Zigmond, S. H. (1992) Thymosin β4 sequester the majority of G-actin in resting human polymorphonuclear leukocytes. *J. Cell Biol. 119*, 1261−1270.